

First Principles Study on the origin of large thermopower in hole doped LaRhO_3 and CuRhO_2

Hidetomo Usui¹, Ryotaro Arita², Kazuhiko Kuroki¹

¹Department of Applied Physics and Chemistry, The University of Electro-Communication, Chofu, Tokyo 182-8585, Japan

²Department of Applied Physics, University of Tokyo, Hongo, Tokyo 113-8656, Japan

Abstract. Based on first principles calculations, we study the origin of the large thermopower in Ni-doped LaRhO_3 and Mg-doped CuRhO_2 . We calculate the band structure and construct the maximally localized Wannier functions, from which a tight-binding Hamiltonian is obtained. The Seebeck coefficient is calculated within the Boltzmann's equation approach using this effective Hamiltonian. For LaRhO_3 , we find that the Seebeck coefficient remains nearly constant within a large hole concentration range, which is consistent with the experimental observation. For CuRhO_2 , the overall temperature dependence of the calculated Seebeck coefficient is in excellent agreement with the experiment. The origin of the large thermopower is discussed.

1. Introduction

The discovery of large thermopower in Na_xCoO_2 [1] and the findings in cobaltates/cobaltites[4, 5, 6, 7, 8] and rhodates[9, 10] that followed have brought up an interesting possibility of finding good thermoelectric materials that have relatively low resistivity. We have recently proposed that the ‘‘pudding-mold’’ type band is the origin for the coexistence of the large thermopower and the low resistivity in this material. [2]. Let us first summarize our idea. Using the Boltzmann’s equation, the thermopower is given as

$$\mathbf{S} = \frac{1}{eT}\mathbf{K}_0^{-1}\mathbf{K}_1 \quad (1)$$

where $e(< 0)$ is the electron charge, T is the temperature, tensors \mathbf{K}_0 and \mathbf{K}_1 are given by

$$\mathbf{K}_n = \sum_{\mathbf{k}} \tau(\mathbf{k})\mathbf{v}(\mathbf{k})\mathbf{v}(\mathbf{k}) \left[-\frac{\partial f(\varepsilon)}{\partial \varepsilon}(\mathbf{k}) \right] (\varepsilon(\mathbf{k}) - \mu)^n. \quad (2)$$

Here, $\varepsilon(\mathbf{k})$ is the band dispersion, $\mathbf{v}(\mathbf{k}) = \nabla_{\mathbf{k}}\varepsilon(\mathbf{k})$ is the group velocity, $\tau(\mathbf{k})$ is the quasiparticle lifetime, $f(\varepsilon)$ is the Fermi distribution function, and μ is the chemical potential. Hereafter, we simply refer to $(\mathbf{K}_n)_{xx}$ as K_n , and $S_{xx} = (1/eT)(K_1/K_0)$ (for diagonal \mathbf{K}_0) as S . Using K_0 , conductivity can be given as $\sigma_{xx} = e^2K_0 \equiv \sigma = 1/\rho$. Roughly speaking for a constant τ , $K_0 \sim \Sigma'(v_A^2 + v_B^2)$, $K_1 \sim (k_B T)\Sigma'(v_B^2 - v_A^2)$ (apart from a constant factor) stand, where Σ' is a summation over the states in the range of $|\varepsilon(\mathbf{k}) - \mu| < \sim k_B T$, and v_A and v_B are typical velocities for the states above and below μ , respectively. If we consider a band that has a somewhat flat portion at the top (or the bottom), which sharply bends into a highly dispersive portion below (above). We will refer to this band structure as the ‘‘pudding mold’’ type. For this type of band with μ sitting near the bending point, $v_A^2 \gg v_B^2$ holds for high enough temperature, so that the cancellation in K_1 is less effective, resulting in $|K_1| \sim (k_B T)\Sigma'v_A^2$ and $K_0 \sim \Sigma'v_A^2$, and thus large $|S| \sim O(k_B/|e|) \sim O(100)\mu\text{V}/\text{K}$. Moreover, the large v_A and the large FS results in a large $K_0 \propto \sigma$ as well, being able to give a large power factor S^2/ρ , which is important for device applications.

In the present study, we focus on a possibly related rhodate LaRhO_3 [3] with Ni doping and CuRhO_2 [15, 16] with Mg doping, in which large thermopower has been observed. In Ni doped LaRhO_3 , the Seebeck coefficient at 300K steeply decreases up to the Ni content of $x = 0.05$, but then stays around $100\mu\text{V}/\text{K}$ up to about $x = 0.3$. On the other hand, the conductivity monotonically grows, resulting in a monotonically increasing power factor (see Fig.2). For CuRhO_2 , the two existing experiments give different results. In ref.[16], the Seebeck coefficient is found to be nearly independent of doping, while it decreases with doping in ref.[15].

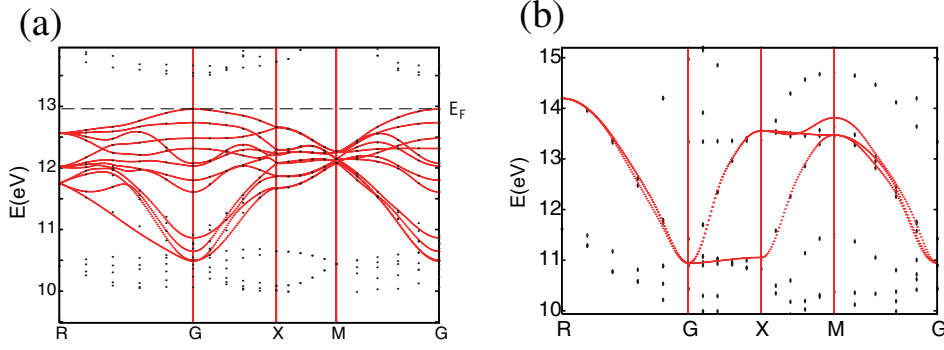


Figure 1. The band structure of the distorted (a) and the ideal (b) structure the tightbinding mode (solid lines) together with the LDA band calculation results (dotted) are shown.

2. Method

LaRhO₃ has an orthorhombic structure, which is distorted to some extent from the ideal cubic perovskite structure. The experimentally determined lattice constants are $a = 5.5242(12)$, $b = 5.7005(12)$ and $c = 7.8968(17)\text{\AA}$ [11]. For comparison, we also calculate the band structure for the ideal cubic perovskite structure, where the lattice constant is taken as $a = 3.940\text{\AA}$. [14] CuRhO₂ has an delafossite structure whose experimental lattice constants are $a = 5.810910$, $c = 32.437162\text{\AA}$. We have obtained the band structure of these materials with the Quantum-ESPRESSO package[12]. We then construct the maximally localized Wannier functions (MLWFs)[13] for the energy window $-1.75eV < \epsilon_k - E_F < -0.64eV$ for the ideal structure of LaRhO₃, $-1.8eV < \epsilon_k - E_F < 0.5eV$ for the distorted structure of LaRhO₃ and $-10eV < \epsilon_k - E_F < 4eV$ for CuRhO₂, where ϵ_k is the eigenenergy of the Bloch states and E_F the Fermi energy. With these effective hoppings and on-site energies, the tight-binding Hamiltonian is obtained, and finally the Seebeck coefficient is calculated using eq.(1). The doping concentration x is assumed to be equal to the hole concentration, and a rigid band is assumed.

3. Results and Discussions

We first present results for LaRhO₃. The calculated band structure for the distorted structure of LaRhO₃ is shown in Fig.1 along with that for the ideal structure. The tightbinding model Hamiltonian for the distorted structure consists of 12 bands (4 Rh per unit cell), while the model for the ideal structure contains three t_{2g} bands. The calculated Seebeck coefficient at 300K is shown in Fig.2 as a function of hole concentration together with the experimental result.[3] Here we assume that the hole concentration n_h is equal to the Ni content. It can be seen that the Seebeck coefficient steeply decreases with doping with $n_h < 0.05$, but stays nearly constant for $n_h > 0.1$ for the distorted structure in particular. As a result the (normalized) power factor monotonically grows with doping, which is at least in qualitative agreement with the

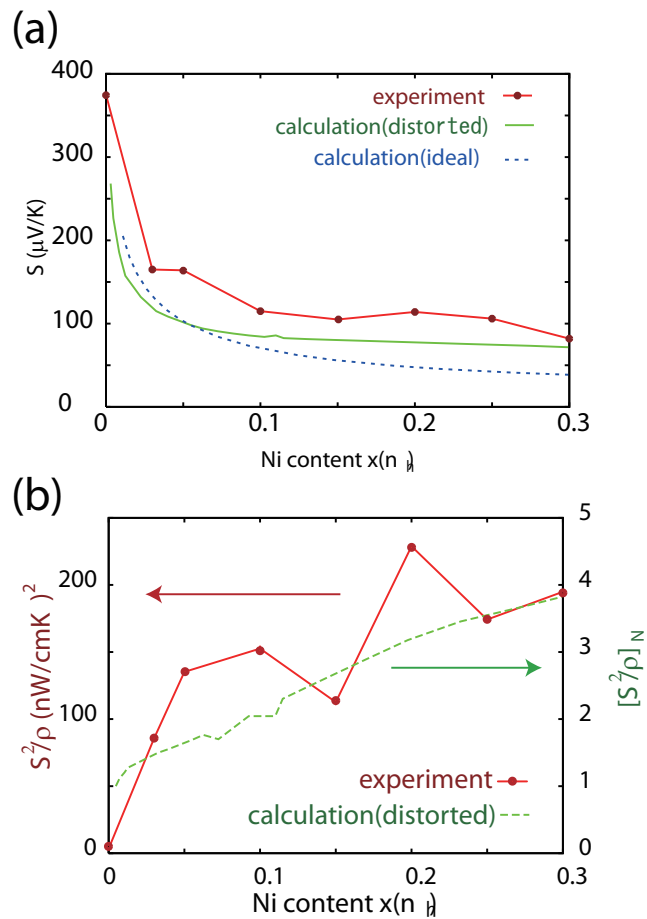


Figure 2. (a) Seebeck coefficient for the distorted (green) and the ideal (blue) structure. The red line is the experimental result.[3] (b) Power factor of the distorted structure normalized at $n_h = 0$. The red line is the experimental data.[3]

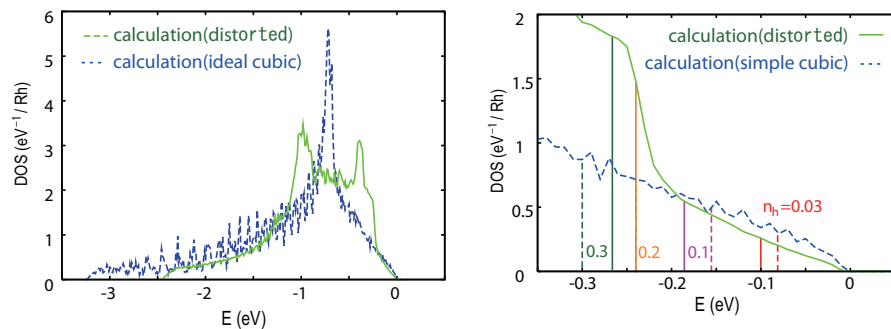


Figure 3. DOS of distorted (green) and ideal (blue) structures. The right panel is a blow up of the left.

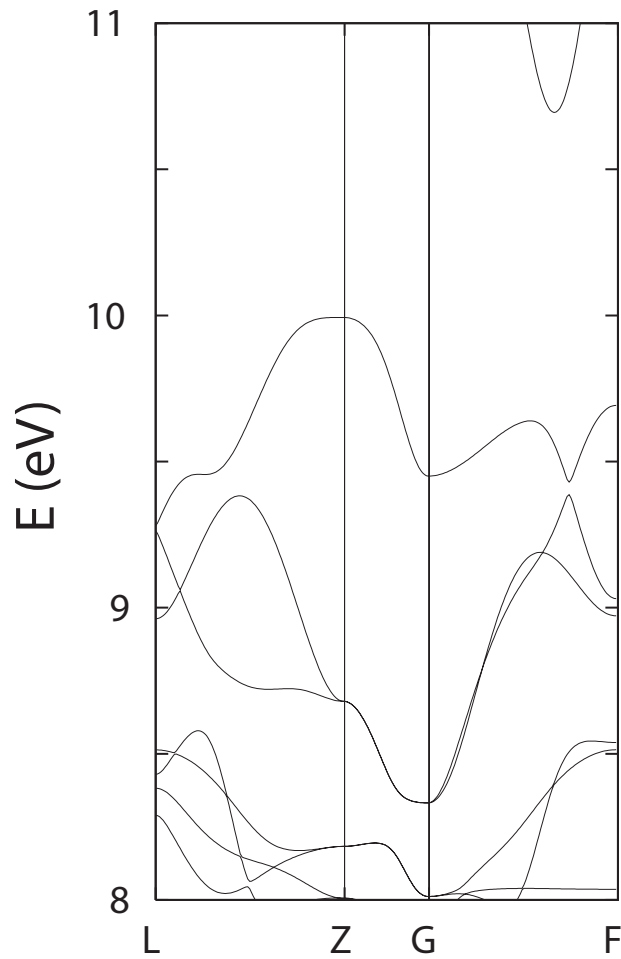


Figure 4. Tightbinding band obtained via maximally localized Wannier orbitals

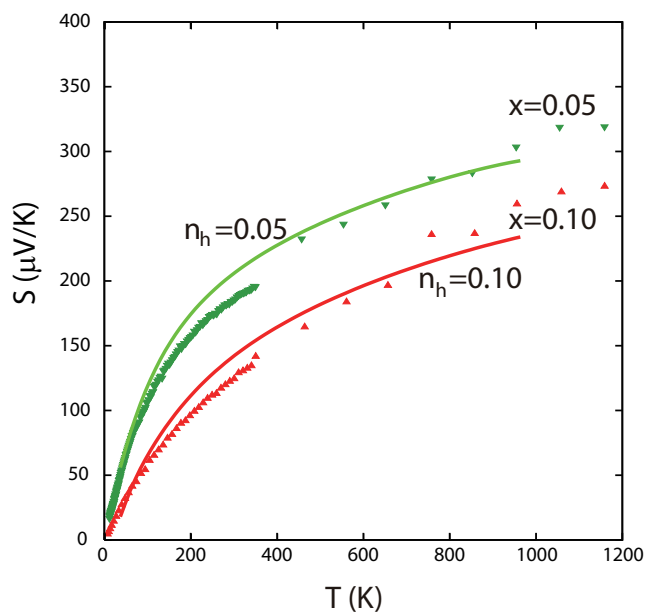


Figure 5. Calculation result of the Seebeck coefficient for CuRhO_2 with the hole concentration of $n_h = 0.05$ and $n_h = 0.1$. The experimental data are from ref.[15]

experimental observation.

Now, in order to understand this peculiar hole concentration dependence of the Seebeck coefficient, we now turn to the density of states (DOS). The comparison of the DOS between the two structures is shown in Fig.3. The DOS at the band top is larger for the ideal case since the three bands are degenerate. Thus, for low doping, E_F stays closer to the band top for the ideal structure, resulting in a larger Seebeck coefficient. This is a typical example where the multiplicity of the bands lead to an enhanced thermopower, i.e., the larger the number of bands, the closer the E_F to the band top. In the case of the distorted structure, as the hole concentration increases, E_F lowers and hits the portion of the band with a large DOS (Fig.3left). Therefore, E_F hardly moves with doping, resulting in a slow decrease of the Seebeck coefficient. A large DOS region lies in a lower energy regime in the ideal structure, and therefore the Seebeck coefficient continues to decrease with doping (up to a larger doping concentration). The large Seebeck coefficient of about $80\mu\text{V}/\text{K}$ in the distorted structure can be considered as due to the flatness of the top of the bands (around the Γ point), i.e., the pudding mold type band.

We now move on to CuRhO_2 . The calculated band structure is shown in Fig.4. Around the Γ point, there is again a pudding mold type band, whose top is very flat. The calculation result of the Seebeck coefficient as a function of temperature is shown in Fig.5. We find excellent agreement with the experiment in ref.[15] in a wide temperature range and for the Mg content $x = 0.05$ and $x = 0.1$. On the other hand, in ref.[16], the Seebeck coefficient is nearly independent on x . The origin of the discrepancy between this experiment and the present calculation remain as a future problem.

4. Conclusion

To conclude, we have studied the origin of the large thermopower in LaRhO_3 and CuRhO_2 . From the first principles band calculation results, a tightbinding model is obtained via the maximally localized Wannier orbitals, and the Seebeck coefficient is calculated using the tightbinding model. In both materials, the large value of the Seebeck coefficient can be considered as due to the flatness of the top of the bands i.e., the pudding mold type band. For LaRhO_3 in particular, the Seebeck coefficient barely decreases for the hole concentration of $n_h > 0.1$ in agreement with the experiment, which we attribute to the peculiar uprising of the DOS near the band top.

The authors acknowledge I. Terasaki, S. Shibusaki, and M. Nohara for valuable discussions and providing us the experimental data. Numerical calculation has been done at the Supercomputing Center, ISSP, University of Tokyo. This study has been supported by the Grants in Aid for Scientific Research from the MEXT of Japan and from JSPS.

References

- [1] I. Terasaki, Y. Sasago, and K. Uchinokura, *Phys. Rev. B* **56**, R12686 (1997)
- [2] K. Kuroki and R. Arita, *J.Phys.Soc.Jpn.* **76**, 083707 (2007)
- [3] S. Shibusaki, Y. Takahashi, and I. Terasaki, arXiv:0712.1626.
- [4] S. Li *et al.*, *J. Mater. Chem.* **9** (1999) 1659
- [5] K. Fujita *et al.*, *Jpn. J. Appl. Phys.* **40** (2001) 4644
- [6] S. Hébert *et al.*, *Phys. Rev. B* **64** (2001) 172101
- [7] Y. Miyazaki *et al.*, *J. Phys. Soc. Jpn.* **71** (2002) 491
- [8] M. Lee *et al.*, *Nat. Mater.* **5** (2006) 537
- [9] S. Okada and I. Terasaki, *Jpn. J. Appl. Phys.* **44** (2005) 1834
- [10] Y. Okamoto *et al.*, *J. Phys. Soc. Jpn.* **75** (2006) 023704
- [11] René B. Macquart *et al.*, *Crystal Growth and Design* **6**(6) (2006) 1361-1365
- [12] S. Baroni *et al.*, <http://www.pwscf.org/>.
- [13] N. Marzari and D. Vanderbilt, *Phys. Rev. B* **56**, 12847 (1997); I. Souza *et al.*, *Phys. Rev. B* **65**, 035109 (2002). The Wannier functions are generated by the code developed by A. A. Mostofi *et al.* (<http://www.wannier.org/>)
- [14] F. S. Galasso, *Structure and Properties of Inorganic Solids* (Pergamon, New York, 1970)
- [15] H. Kuriyama, M. Nohara, T. Sasagawa, K. Takubo, T. Mizokawa, K. Kimura, and H. Takagi, *Proc. 25th Int. Conf. on Thermoelectrics* (IEEE, Piscataway, 2006)
- [16] S. Shibusaki, W. Kobayashi, and I. Terasaki, *Phys. Rev. B* **74**, 235110 (2006).